On the Relationship between the Preferred Site of Hydrogen Bonding and Protonation

ARTICLE *in* THE JOURNAL OF PHYSICAL CHEMISTRY A · JULY 2005

Impact Factor: 2.69 · DOI: 10.1021/jp0516994 · Source: PubMed

4 AUTHORS, INCLUDING:

Bun Chan
University of Sydney
78 PUBLICATIONS **939** CITATIONS
SEE PROFILE

José Elguero
Spanish National Research Council
1,502 PUBLICATIONS **22,232** CITATIONS
SEE PROFILE

On the Relationship between the Preferred Site of Hydrogen Bonding and Protonation

Bun Chan,*,† Janet E. Del Bene,*,‡ Jose Elguero,*,§ and Leo Radom*,†

School of Chemistry, University of Sydney, Sydney, NSW 2006, Australia, Department of Chemistry, Youngstown State University, Youngstown, Ohio 44555, and Instituto de Quimica Medica, CSIC, Juan de la Cierva, 3, E-28006 Madrid, Spain

Received: April 3, 2005

Ab initio molecular orbital calculations have been employed to investigate the interactions between a set of basic substrates (B) with H^+ and HF, and the interaction between acids of varying strength (AH^+) with two bases, vinylamine and furan. The preferred site for protonation of the substrates appears to be determined primarily by the ability of the protonated species (BH^+) to delocalize the acquired positive charge. On the other hand, localization of a pair of electrons at a proton-acceptor site of B tends to be more important in determining the preferred site for hydrogen bonding with HF. The behavior of acids stronger than HF lies between these extremes. Consistent with a previously proposed Hammond postulate for complexes, when a substrate (B) interacts with a range of acids (AH^+), proton transfer is generally found to occur when the proton affinity of A is significantly less than that of B. When the proton affinity of A is greater than that of B, a hydrogen-bonded complex is generally formed without proton transfer. Strongest binding (relative to the lowest energy components) occurs when the proton affinities of A and B are comparable. Proton transfer from AH^+ is found to take place in some cases when this would not be predicted on the basis of protonation energies alone, because of specific interactions in the resulting complexes.

Introduction

Hydrogen bonding and protonation are processes that are ubiquitous and of utmost importance in chemical and biological systems. As a result, these reactions have been extensively investigated experimentally and theoretically.[1] Hydrogen bonding and protonation are related phenomena that can both be viewed as acid−base interactions, with hydrogen bonding being a relatively weak interaction, while protonation is very strong. Linear correlations have been observed between proton affinities and hydrogen-bond enthalpies for a set of closely related bases.[2] Moreover, several authors have compared the basicity scales obtained in solution for Brønsted basicity and hydrogen-bonding basicity.[2] Legon investigated hydrogen bonding and protonation in a series of complexes formed between hydrogen halides and aliphatic amines. On the basis of his microwave spectroscopic data, several criteria for determining when hydrogen-bond formation leads to proton transfer have been proposed.[3,4] Low-temperature matrix isolation spectroscopy has also been used to examine the process of proton transfer in hydrogen-bonded complexes.[5] Depending on the complex, the extent of proton transfer can be influenced by the nature of the matrix material.[6] Limbach and co-workers have used temperature effects to induce proton transfer in hydrogen-bonded complexes, and have related the degree of proton transfer to changes in NMR spin−spin coupling constants involving the hydrogen-bonded atoms.[7] Their observations were subsequently supported by ab initio studies of changes in coupling constants as a function of proton position and hydrogen-bond type.[8] Other theoretical studies of hydrogen bonding and proton transfer have also been reported.[9] Recently, theoretical studies have predicted that hydrogen bonding by enzymes can facilitate the radical rearrangement step in coenzyme B_{12}-mediated reactions through a partial-proton-transfer mechanism,[10] and this has been supported experimentally.[11] Finally, on the basis of structure correlations from X-ray crystallographic data, Bürgi and Dunitz proposed that hydrogen-bond formation in general could be regarded as the incipient stage of the proton-transfer process.[12] All of these observations suggest that protonation data should be useful for predicting the conditions under which hydrogen-bond formation leads to proton transfer. However, this may not always be the case.

What happens when a Brønsted acid $A-H^+$ encounters a Brønsted base B? The long-range interaction between the two moieties is attractive, so that as they approach, a hydrogen-bonded complex $A-H^+\cdots B$ is formed. In some cases, proton transfer can occur, resulting in an alternative hydrogen-bonded complex $A\cdots{}^+H-B$. According to the Hammond postulate for complexes, when two sets of reactants (X−Y + Z) or (X + Y−Z) interact to form a common stable complex (X···Y···Z), the complex will generally resemble the set of reactants that has the lower energy.[13] If this postulate is applied to the interaction between $A-H^+$ and B, an $A-H^+\cdots B$ hydrogen-bonded complex should be observed if the proton affinity of A is greater than that of B (Figure 1a). On the other hand, proton transfer to form the hydrogen-bonded complex $A\cdots{}^+H-B$ would be expected if the proton affinity of A is less than that of B (Figure 1c). In this situation, the energy for the complexation reaction $A-H^+ + B \rightarrow A\cdots{}^+H-B$ (E_1) is determined primarily by the difference in the proton affinities of A and B (ΔPA). In this case, it would be more appropriate to calculate the hydrogen-bond energy with respect to A plus ^+H-B (E_2) rather than with respect to $A-H^+ + B$ (E_1). In this paper, we shall refer to E_2 as the retro-binding energy. If A and B have

* Address correspondence to the authors at the following e-mail addresses: chan_b@chem.usyd.edu.au; jedelbene@ysu.edu; iqmbe17@iqm.csic.es; radom@chem.usyd.edu.au.

† University of Sydney.

‡ Youngstown State University.

§ CSIC.

10.1021/jp0516994 CCC: $30.25
Published on Web 05/26/2005

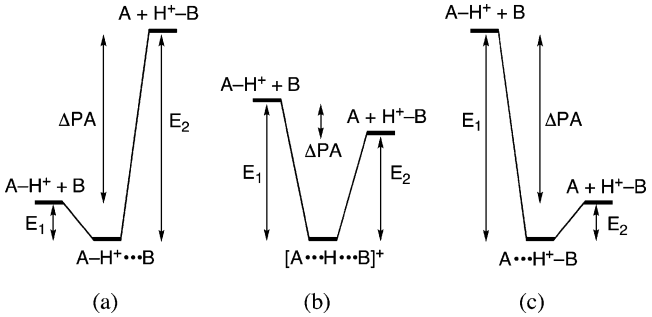

Figure 1. Hydrogen-bonded complex formed from A−H$^+$ plus B: (a) the proton affinity of A is much greater than that of B, (b) A and B have similar proton affinities, and (c) the proton affinity of B is much greater than that of A.

similar proton affinities (Figure 1b), the details of the interaction that occurs can be significantly influenced by specific characteristics of the possible products. Nevertheless, a strong hydrogen bond would be expected. In other words, E_1 would be similar in magnitude to E_2 and both are likely to be substantially larger than the binding energies relative to the lowest energy components in parts a and c of Figure 1 where ΔPA is much larger.

Several important problems and questions are associated with the very general and simplistic picture given above. Do Brønsted basicities and hydrogen-bond complexation energies always correlate? If not, under what circumstances are they different? If a molecule has multiple protonation sites, does the preferred site of protonation always coincide with the preferred site for hydrogen bonding? If not, then what factors favor protonation at one site and hydrogen bonding at another? How are the answers to these questions related to the acidity and/or the nature of the hydrogen-bond donor, and the basicity and/or the nature of the hydrogen-bond acceptor? Are there other factors that should be considered when attempting to answer these questions?

The aim of the present study is to address the questions raised above by examining in detail relationships between hydrogen bonding and protonation. To do this, high-level ab initio molecular orbital calculations have been carried out on a variety of complexes in which protonation and/or hydrogen bonding occur. The acidities of the donor species in these complexes span a range of more than 1000 kJ mol^{-1}; the basicities of the acceptors span a similar range. The acceptor moieties include species that have lone pairs of electrons and/or π-electron systems as potential basic sites.[14]

Computational Details

Standard ab initio molecular orbital calculations[15] were carried out with the GAUSSIAN 03[16] program. Geometries of monomers and complexes were obtained at the MP2/6-31+G(d,p) level of theory. Vibrational frequencies were computed to establish that all structures correspond to local minima on their potential surfaces. Improved energies for complex formation were obtained at MP2/aug′-cc-pVTZ. A counterpoise correction to account for possible basis set superposition error (BSSE) was not employed since it is still an open question whether this will necessarily lead to better binding energies at this level of theory.[17] Geometrical parameters and reaction energies in the text refer to values calculated at these levels of theory.

To assess the performance of the method used, proton affinities of the substrates (B) and of the conjugate bases of the acids (A) were computed and compared with experimental proton affinities at 298.15 K and 1 atm. For these comparisons,

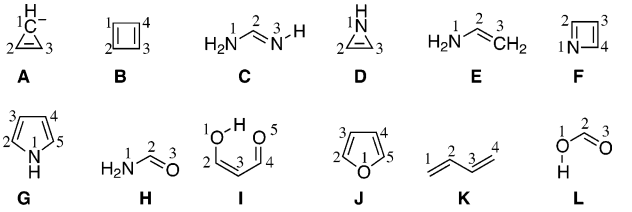

Figure 2. Substrates for protonation and hydrogen bonding with HF.

computed proton affinities ($-\Delta H^{298.15}$ for the reaction B + H$^+$ → BH$^+$) were obtained by adding zero-point vibrational and thermal corrections to the MP2/aug′-cc-pVTZ electronic energies. The zero-point energies were obtained from MP2/6-31+G-(d,p) frequencies scaled by 0.9608, and the thermal vibrational energies were computed from the same frequencies scaled by 1.0084.[18]

Comparisons of computed reaction energies involving the various acids and bases included in this study are based on reaction energies calculated without zero-point and thermal corrections. Protonation energy is defined as the electronic energy change for the reaction X + H$^+$ → X−H$^+$, where X represents the substrate. Similarly, the complexation/binding energy is defined as the electronic energy change for the reaction X + Y → X···Y, where X and Y are components of the complex X···Y. Since all of these reactions are exothermic, the signs of the reaction energies are negative. However, for ease of discussion, the absolute values of these energies will be compared. This means that for the reaction X + H$^+$ → XH$^+$, X is more basic when the reaction energy has a greater negative value, or a greater absolute value.

Substrate Protonation and Hydrogen-Bond Formation with HF

In the initial phase of this study, 12 bases (**A**−**L** in Figure 2) were selected as substrates, and the structures and binding energies of the complexes formed by these bases with H$^+$ and HF were computed. All of the substrates possess π-electrons that can potentially act as proton and/or hydrogen-bond acceptor sites. Some of the substrates also contain electronegative elements (N and O) that have isolated and/or delocalized lone-pairs of electrons.

A. Protonation. The calculated protonation energies of **A**−**L** are summarized in Table 1, together with calculated and experimental proton affinities. The calculated proton affinities provide reasonable estimates of the experimental values, although a relatively large error is found for pyrrole (**G**). Nevertheless, the computed PAs reproduce the order of the experimental values. In Table 1 the molecules are arranged in descending order of protonation energy, that is, in order of decreasing basicity. Cyclopropenyl anion (**A**) has by far the highest protonation energy due to its negative charge, and it is therefore the strongest base. Cyclobutadiene (**B**) is the strongest neutral base. Interestingly, 1,3-butadiene (**K**), which prefers to be protonated at C1, has a much smaller protonation energy than **B**, its cyclic analogue. The π-electrons of **K** are delocalized, as reflected in the short C2−C3 single-bond length of 1.458 Å (Figure 3), as compared with a typical C−C single bond (e.g., 1.531 Å in ethane). On the other hand, the π-electrons of **B** are not significantly delocalized, as indicated by the C2−C3 bond length of 1.566 Å, which is even slightly longer than that of a typical C−C single bond. The long C2−C3 bond is reflective of the antiaromaticity of **B**. When protonated, however, both **B** and **K** give allyl cation systems that are stabilized by delocalization of the positive charge (Figure 3). Consequently, **B** gains

TABLE 1: MP2/Aug′-cc-pVTZ//MP2/6-31+G(d,p) Protonation Energies and Computed and Experimental Proton Affinities (kJ mol^{-1})[a,b]

	atom where protonation occurs[c]					
substrate	1	2	3	5	PA_{calc}[d]	PA_{expt}[e]
A	−1783.3[g]				1748.9	
B[i]	−976.5				943.6	
C[f]	−843.9		*−970.8*[g]		940.4	
D	−951.5[g]	*−963.0*			929.8	
E[f]	−884.9		*−941.7*		911.8	898.9
F	−898.1	−877.0	*−899.4*		870.6	
G[g]	−797.7[g]	*−871.9*	−851.2		843.6	875.4
H[f]	−783.6		*−853.7*		824.0	822.2
I			−795.0	*−835.3*	806.2	
J[g]	−702.2	*−816.7*	−766.5		789.4	803.4
K[h]	−801.6				775.7	783.4
L	−677.6		*−760.4*		732.7	742.0

[a] For substrates with more than one site of protonation, the protonation energy of the most basic site is shown in italics. [b] The substrates and protonated species have C_s symmetry unless otherwise noted. [c] See Figure 2 for numbering of atoms. [d] Calculated proton affinities are $-\Delta H^{298.15}$ values based on the protonation energy at the preferred protonation site. [e] Experimental proton affinities obtained from the NIST Chemistry WebBook.[19] [f] C_1. [g] C_{2v}. [h] C_{2h}. [i] D_{2h}.

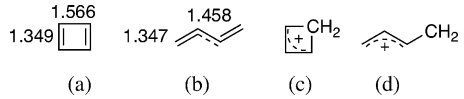

Figure 3. Calculated C−C bond lengths (Å) in (a) cyclobutadiene (**B**) and (b) 1,3-butadiene (**K**) and (c, d) delocalization of positive charge in the corresponding protonated forms.

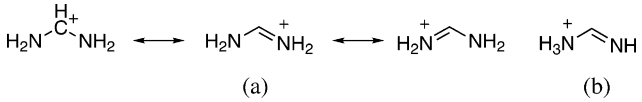

Figure 4. Protonation of formamidine (**C**) at (a) N3, where the positive charge is delocalized, and (b) at N1, where the charge is localized at N1.

extra stability upon protonation, and is a much stronger base than **K**, which does not enjoy the same advantage upon protonation.

Formamidine (**C**) can be protonated at either N3 or N1, with protonation at N3 preferred by 26.9 kJ mol^{-1}. Protonation at N3 (Figure 4a) occurs at the in-plane nitrogen lone-pair. The resulting amidinium cation is planar, with the positive charge stabilized by delocalization over the two nitrogen atoms that are equivalent in the cation (Figure 4). On the other hand, protonation at N1 (Figure 4b) leads to a formally localized positive charge at N1. Molecules analogous to **C**, namely formamide (**H**) and formic acid (**L**), show similar behavior toward protonation. Both preferentially protonate at an in-plane lone-pair on the carbonyl oxygen O3 rather than at N1 or O1. The differences between the protonation energies at sites 3 and 1 for **H** and **L** are 70.1 and 82.8 kJ mol^{-1}, respectively.

The protonation energies of **C**, **H**, and **L** decrease in the order **C** > **H** > **L**, consistent with N being a better proton acceptor than O. The protonation order **C** > **H** > **L** is also consistent with the relative stabilization energies of X−CH−Y$^+$ carbocations by adjacent NH_2 and OH groups, NH_2 being a better π-donor than OH. This makes $NH_2CHNH_2^+$ relatively favored over NH_2CHOH^+, which in turn is favored over $HOCHOH^+$.

1*H*-Azirine (**D**), and its acyclic analogue vinylamine (**E**), can protonate at the nitrogen or at a carbon (C3 in the case of **E**), with carbon being the preferred protonation site. The differences between the nitrogen and carbon protonation energies for **D** and **E** are 11.5 and 56.8 kJ mol^{-1}, respectively. The preference for carbon protonation arises from the stability gained from delocalization of the positive charge, similar to that illustrated for N3-protonated formamidine in Figure 4.

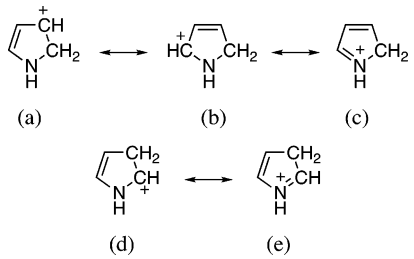

Figure 5. Resonance structures for protonation of 1*H*-pyrrole (**G**) at C2 (structures a−c),and at C3 (structures d and e).

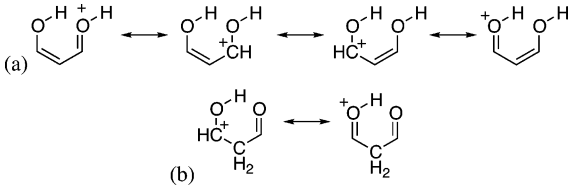

Figure 6. Resonance structures for protonation of malonaldehyde (**I**) at (a) O5 and (b) C3.

Azete (**F**) can be protonated at three sites, N1, C2, or C3. The protonation energies at N1 and C3 are comparable, with C3 slightly preferred by 1.3 kJ mol^{-1}. C2 protonation leads to a cation that is approximately 21 kJ mol^{-1} less stable. Azete (**F**) is structurally similar to cyclobutadiene (**B**) and is also antiaromatic. The preference for C3 protonation may be attributed to the better delocalization of the positive charge in the cation when protonation occurs at this site.

Protonation of 1*H*-pyrrole (**G**) can occur at N1, C2, or C3, with the protonation energies decreasing in the order C2 > C3 > N1. C2 protonation is favored over C3 by 20.7 kJ mol^{-1}, while C3 protonation is favored over N1 by 53.5 kJ mol^{-1}. Protonation at N1 is least favorable because it results in a formally localized charge at N1, whereas protonation at either C2 or C3 leads to charge delocalization. The preference for protonation at C2 over C3 can be rationalized in terms of the resonance structures shown in Figure 5. The C2-protonated product has three resonance structures (a), (b), and (c). The C3-protonated product has only two, (d) and (e), which are similar to (b) and (c) of the C2-protonated cation. Thus, charge delocalization considerations suggest that the C3 cation is the most stable species.

Furan (**J**) exhibits behavior toward protonation similar to that of its nitrogen analogue pyrrole (**G**). Thus, **J** can protonate at O1, C2, or C3, with the relative stabilities of the protonated species decreasing in the order C2 > C3 > O1. C2 protonation is 50.2 kJ mol^{-1} more favorable than C3 protonation, whereas protonation at C3 is more favorable than O1 by 64.3 kJ mol^{-1}. The order C2 > C3 > O1 can be explained by using the same arguments as were applied to pyrrole. Protonation at C2 leads to a more delocalized charge than protonation at C3, and protonation at O1 gives a formally localized charge at that atom.

Protonation of malonaldehyde (**I**) can occur at C3 and O5, with O5 preferred by 40 kJ mol^{-1}. The preference for O5 protonation is supported by the resonance structures depicted in Figure 6. The positive charge on the O5-protonated species is highly delocalized over two C atoms and two O atoms, whereas the positive charge on the C3-protonated product is only delocalized over one C atom and one O atom. Thus, the greater delocalization of charge favors O5 as the more basic site.

TABLE 2: MP2/aug′-cc-pVTZ//MP2/6-31+G(d,p) Binding Energies with HF (kJ mol^{-1})[a,b]

	atom where interaction with HF occurs[c]			
substrate	1	2	3	5
A	*−251.1*[d]	−66.5[d]		
B	−22.9[d]			
C	−33.9		*−67.4*	
D	−60.6[d]	−16.7[d]		
E	−43.2		−30.8	
F	*−49.6*[d]		−5.0[d]	
G			−28.8	
H	−21.6		*−55.1*[d]	
I	−28.2		−13.5	*−39.1*[d]
J	*−25.9*[e]		−20.6	
K	−20.9			
L	−21.7		*−45.1*[d]	

[a] For substrates with more than one site of binding, the most negative binding energy is shown in italics. [b] The hydrogen-bonded complexes have C_1 symmetry unless otherwise noted. [c] In this table, hydrogen-bond formation is listed as occurring at a particular C atom, but in some cases, bonding occurs at a C=C bond, as noted in the text. See Figure 1 for numbering of atoms. [d] C_s. [e] C_{2v}.

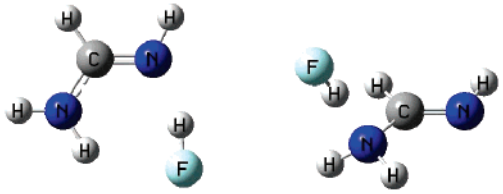

(a) (b)

Figure 7. Hydrogen-bonded complexes of formamidine (**C**) with HF: (a) the preferred complex at N3 and (b) the higher energy complex at N1.

B. Hydrogen Bonding with HF. The calculated binding energies of complexes formed by the bases **A**−**L** with HF are listed in Table 2. When HF interacts with the cyclopropenyl anion (**A**) at C1, proton transfer occurs. The reaction is highly exothermic (by −251.1 kJ mol^{-1}), and the complex formed has F^- bonded to cyclopropene. A second π-complex in which HF is hydrogen bonded to **A** at the center of the C2=C3 bond has also been located on the potential surface. This complex lies 184.6 kJ mol^{-1} higher in energy than the complex formed at C1. For the other two hydrocarbon bases **B** and **K**, only one hydrogen-bonded complex with HF is found, corresponding to interaction through the π system of the C1=C2 double bond.

Formamidine (**C**) forms hydrogen-bonded complexes with HF at N1 and N3, with N3-complexation being preferred by 33.5 kJ mol^{-1}. The significant preference for hydrogen bonding at N3 may be attributed to two factors. First, the lone pair of electrons is localized on N3 in the symmetry plane, whereas the N1 lone pair is somewhat delocalized into the π system. The concentrated electron density at N3 favors the formation of an F−H···N3 hydrogen bond. The second factor that favors hydrogen bonding at N3 is the formation of a bridging hydrogen-bonded structure in which the HF molecule also acts as a proton acceptor from an N1−H bond, forming a second, distorted N1−H···F hydrogen bond. The two complexes are displayed in Figure 7.

The two molecules structurally related to formamidine (**C**), namely, formamide (**H**) and formic acid (**L**), form hydrogen-bonded complexes with HF that are structurally similar to those formed with formamidine. Hydrogen bonding with HF as the proton donor occurs preferentially at the in-plane lone-pair of electrons of the carbonyl oxygens, and the resulting complexes have bridging structures in which N1−H or O1−H are proton donors for a second distorted hydrogen bond with HF. Hydrogen bonding at O3 is favored over N1 in **H** by 33.5 kJ mol^{-1}, and over O1 in **L** by 23.4 kJ mol^{-1}.

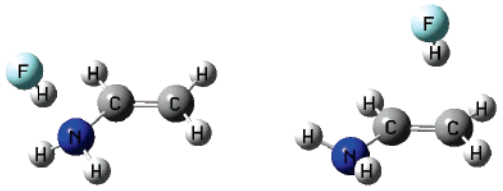

(a) (b)

Figure 8. The hydrogen-bonded complexes of vinylamine (**E**) with HF: (a) the preferred complex at N1 and (b) the higher energy π-complex at C2=C3.

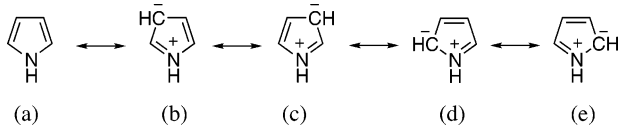

(a) (b) (c) (d) (e)

Figure 9. Resonance structures for 1*H*-pyrrole (**G**).

Two complexes of 1*H*-azirine (**D**) with HF were found on the potential surface, one at N1 and the other at the C2=C3 double bond. The complex at N1 is favored by 43.9 kJ mol^{-1}. Similarly, vinylamine (**E**), the acyclic analogue of **D**, forms hydrogen-bonded complexes with HF at N1 and at the C2=C3 double bond. The N1-complex is preferred over the π-complex of vinylamine by 12.4 kJ mol^{-1}, even though the lone-pair on N1 is delocalized to some extent into the π system. Nevertheless, a nearly linear F−H···N1 hydrogen bond is formed, as shown in Figure 8. In addition, HF forms a π hydrogen bond at C2=C3, with the FH molecule pointing toward C3. These complexes illustrate that, in general, hydrogen bonding of HF is more favorable when the electron density at a proton-acceptor site is localized at an atom such as C^-, N, or O rather than located in a π-electron system.

Azete (**F**) forms hydrogen bonds with HF at N1 and C3, with N1 being the preferred site by 44.6 kJ mol^{-1}. A hydrogen-bonded complex of pyrrole (**G**) with HF was found only at C3. The absence of a complex through N1 is presumably due to the extensive delocalization of the N1 lone-pair of electrons over the diene system (Figure 9), thereby decreasing the basicity at N1. That π-complexation occurs at C3 can be explained in terms of resonance structures (b) and (c), which provide the strongest electrostatic interaction with HF by maximizing charge separation within the molecule. In contrast to pyrrole, furan (**J**) forms two hydrogen-bonded complexes with HF, one through a lone pair at O1, and the other through the π system at C3. Hydrogen bonding at O1 is favored over C3 by 5.3 kJ mol^{-1}, most probably because of the greater electron density at this heteroatom.

Malonaldehyde (**I**) forms hydrogen-bonded complexes with HF at O1, C3, and O5. The relative stabilities of the complexes decrease in the order O5 > O1 > C3. The O5 complex is 10.9 kJ mol^{-1} more stable than the O1 complex, while O1 is 14.7 kJ mol^{-1} more stable than C3. The same arguments used to explain the ordering for formamidine (**C**) and vinylamine (**E**) can be applied to malonaldehyde.

C. Protonation versus Hydrogen Bonding. A comparison of results in Tables 1 and 2 reveals that cyclopropenyl anion (**A**), cyclobutadiene (**B**), formamidine (**C**), formamide (**H**), malonaldehyde (**I**), 1,3-butadiene (**K**), and formic acid (**L**) preferentially protonate and form hydrogen-bonded complexes

TABLE 3: MP2/aug′-cc-pVTZ//MP2/6-31+G(d,p) Protonation Energies[a] and Computed[a] and Experimental[b] Proton Affinities (kJ mol^{-1}) of the Conjugate Bases A$^{(n-1)+}$

A−H^{n+}	A$^{(n-1)+}$	E_{prot}	PA_{calc}	PA_{expt}	$PA_{calc} - PA_{expt}$
HF−H$^+$	HF	−503.3	483.4	484.0	−0.6
HCl−H$^+$	HCl	−571.2	553.4	556.9	−3.5
HBr−H$^+$	HBr	−596.0	580.6	584.2	−3.6
H_2O−H$^+$	H_2O	−711.5	683.5	691.0	−7.5
HCN−H$^+$	HCN	−727.0	703.1	712.9	−9.8
HNC−H$^+$	HNC	−801.4	777.7	772.3	5.4
LiCl−H$^+$	LiCl	−832.7	818.0	827.0	−9.0
H_3N−H$^+$	NH_3	−881.5	848.6	853.6	−5.0
MeH_2N−H$^+$	NH_2Me	−928.4	895.5	899.0	−3.5
LiCN−H$^+$	LiCN	−949.6	926.4		
Me_2HN−H$^+$	$NHMe_2$	−961.9	928.2	929.5	−1.3
Me_3N−H$^+$	NMe_3	−978.3	944.1	948.9	−4.8
NaCN−H$^+$	NaCN	−997.9	974.6		
LiNC−H$^+$	LiNC	−1018.7	996.0		
Br−H	Br$^-$	−1362.1	1350.1	1353.5	−3.4
Cl−H	Cl$^-$	−1401.1	1387.0	1395.0	−8.0
CN−H	CN$^-$ (N)	−1411.8	1388.8		
NC−H	CN$^-$ (C)	−1486.2	1463.3	1468.2	−4.9
F−H	F$^-$	−1560.9	1540.9	1554.0	−13.1

[a] Proton affinities are $-\Delta H^{298.15}$ values. [b] Obtained from NIST Chemistry WebBook.[19]

with HF at the same basic site. In contrast, the preferred sites for protonation and hydrogen bonding with HF are different for 1*H*-azirine (**D**), vinylamine (**E**), azete (**F**), pyrrole (**G**), and furan (**J**). The preferred site for protonation of a substrate is determined by the stability of the resulting cation, which depends strongly on the ability of that structure to delocalize the acquired positive charge. On the other hand, the preferred site for hydrogen bonding is influenced more by electrostatic interactions and bond formation through an electron pair, and corresponds generally to the site with the more localized negative charge. When these characteristics are found at different sites, then hydrogen bonding and protonation may occur at different sites in a molecule. In what follows we will further investigate this difference.

The protonation energy of any given molecule (B) is a well-defined thermodynamic quantity that depends solely on the nature of the base. Similarly, the energy of hydrogen-bond formation is well-defined, but it depends not only on the basicity of the substrate (B), but also on the proton-donating ability of the donor moiety (AH$^+$). Since it has been shown above that for some molecules the site of protonation is different from that of hydrogen bonding with HF, it should be expected that a change in the acidity of the donor may change the preferred interaction site with a base and the reaction that occurs. To investigate this possibility, vinylamine (**E**) and furan (**J**) have been chosen as the substrates on which to examine reactions with acids of various strengths. The choice of these two substrates is based on the fact that in both these cases the preferred sites for protonation and for hydrogen bonding with HF are different. In addition, since the protonation energies of these molecules are also significantly different, it may be anticipated that they will show different behavior toward the same set of acids. The set of acids chosen to investigate protonation or hydrogen bonding with vinylamine (**E**) and furan (**J**) are listed in Table 3 as (A−H^{n+}). Their conjugate bases (A$^{(n-1)+}$) are also listed, together with their computed and experimental proton affinities. With one exception, the calculated proton affinities underestimate the experimental values, as has been observed previously for MP2 calculations with reasonably large basis sets.[20] However, the agreement between computed and experimental proton affinities is reasonable, and the use of MP2/aug′-cc-pVTZ energies should not lead to significant errors in a qualitative analysis of the computed results.

TABLE 4: MP2/aug′-cc-pVTZ//MP2/6-31+G(d,p) Binding Energies[a] of Hydrogen-Bond Donors (A−H^{n+}) to Vinylamine (kJ mol^{-1})[b]

	site of binding	
A−H^{n+}	N1	C3
H$^+$	−884.9[c]	−941.7[c]
HF−H$^+$	−428.9 (**−47.3**)	−483.7 (**−45.3**)[c]
HCl−H$^+$	−347.5 (**−33.8**)	−401.5 (**−30.9**)
HBr−H$^+$	−325.6 (**−36.6**)	−379.6 (**−33.9**)
H_2O−H$^+$	−252.7 (**−79.2**)	−305.6 (**−75.3**)[c]
HCN−H$^+$	−243.6 (**−85.8**)	−294.5 (**−79.8**)[c]
HNC−H$^+$	−173.1 (**−89.7**)	−223.3 (**−83.0**)[c]
LiCl−H$^+$	−187.3 (**−135.1**)	−235.9 (**−126.9**)[c]
H_3N−H$^+$	−103.3 (**−99.9**)	
MeH_2N−H$^+$	−93.0 (**−136.5**)	
LiCN−H$^+$	−114.3 (**−179.1**)	−71.9 (**−79.8**)
Me_2HN−H$^+$	−87.1 (**−164.1**)	−77.6 (**−97.7**)
Me_3N−H$^+$	−83.6 (**−177.0**)	−76.3 (**−112.9**)
NaCN−H$^+$	−90.9 (**−203.9**)	−63.4 (**−119.5**)
LiNC−H$^+$	−63.6 (**−197.3**)	−53.9 (**−130.9**)
Br−H	−31.7 (**−508.9**)	−25.9 (**−446.3**)
Cl−H	−31.6 (**−547.8**)	−24.8 (**−484.2**)
CN−H	−40.5 (**−567.3**)	−31.0 (**−501.1**)
NC−H	−23.3 (**−624.6**)	−19.5 (**−564.0**)
F−H	−43.2 (**−719.2**)	−30.8 (**−650.0**)

[a] Binding energies in regular font are relative to vinylamine plus A−H^{n+}, those in bold are relative to protonated vinylamine at the corresponding atom plus A$^{(n-1)+}$. [b] The complexes have C_1 symmetry unless otherwise noted. [c] C_s.

The hydrogen-bond donors that are listed in Table 3 are arranged in ascending order of proton affinities of the conjugate bases, i.e., descending order of acidities. The strongest (gas-phase) acids are listed at the top of the table, beginning with H_2F^+; the weakest acid is HF at the bottom. It is of interest to examine whether this order is maintained in the hydrogen-bond energies of the acids when they interact with vinylamine or furan.

Reactions of Vinylamine with Acids

The reaction energies for complexes formed between the various acids and vinylamine are reported in Table 4. In some cases, complexation leads to proton transfer to vinylamine, so binding energies relative to protonated vinylamine plus the conjugate base (E_2 in Figure 1) are also given in bold. As noted before, these energies are designated as retro-binding energies. The energy of protonation of vinylamine by H$^+$ is also included for comparison. In general, the binding energy (E_1) becomes smaller with decreasing acidity of the proton donors, whereas the retro-binding energy (E_2) becomes larger. This is consistent with the Hammond postulate for complexes (Figure 1).

A. Strong Acids: H_2F^+ to LiClH$^+$. Reaction of vinylamine (**C**) with the strongest acids as hydrogen-bond donors leads to proton transfer at N1 and at C3, as anticipated (cf. Figure 1c). This is exemplified by the optimized structures of the complexes formed with H_2F^+, shown in Figure 10. Proton transfer to N1 results in a complex stabilized by an N1−H···F hydrogen bond. Interestingly, C3-protonation with H_2F^+ is followed by a migration of HF to N1, again with the formation of an N1−H···F hydrogen bond.

The complexes formed between vinylamine and the remaining strong acids (AH$^+$) exhibit similar behavior, that is, proton transfer to N1 or C3 occurs with subsequent formation of an N1−H···X hydrogen bond. C3 protonation is favored over N1

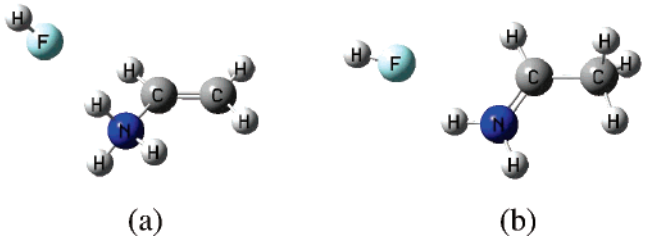

Figure 10. Complexes resulting from the reaction of vinylamine with H_2F^+: (a) protonation at N1 and (b) protonation at C3 followed by migration of HF to form a complex at N1.

protonation, consistent with the greater proton affinity of C3 when H^+ is the protonating agent. Relative to vinylamine plus the protonating acids, reaction energies corresponding to proton transfer to C3 are greater than those for proton transfer to N1 by 54.8 (H_2F^+), 54.0 (H_2Cl^+), 54.0 (H_2Br^+), 52.9 (H_3O^+), 50.9 (HCN−H^+), 50.2 (HNC−H^+), and 48.6 (LiClH$^+$) kJ mol^{-1}. These numbers reflect the differences in energy between the C-protonated and N-protonated species, moderated by the differential strength of the N1−H···X hydrogen bonds in the resultant N1 and C3 complexes (cf. Figure 10). The similarity in these values is striking and indicates that the differences in the hydrogen-bond strengths do not vary significantly as X is varied. Similar observations may be made for the retro-binding energies, which provide a direct measure of the binding energies associated with N1−H···X hydrogen bonding.

Consistent with Figure 1, the reaction energies associated with protonation and subsequent hydrogen-bond formation with vinylamine decrease with the acidity of the protonating acid, with the single exception being the reversal of stabilities of complexes formed when LiClH$^+$ and HNC−H^+ are the protonating acids. LiClH$^+$ is the least acidic among the strong acids based on the protonation energy of its conjugate base, but its reaction energy with vinylamine is somewhat greater than that of the stronger acid HNC−H^+. Some insight into this reversal can be gained by considering the retro-binding energies reported in Table 4. Although the retro-binding energies of the complexes with strong acids generally increase with increasing basicity of the conjugate base, the retro-binding energies for LiClH$^+$ are significantly greater than retro-binding energies for HCN−H^+. This may be attributed to the formation of a very strong N1−H···Cl hydrogen bond due to the large negative charge on Cl, and a favorable head-to-tail alignment of the dipole moment of LiCl with the N1−H bond dipole, particularly in the complex protonated at N1. Finally, it is noteworthy that for each protonating acid, the retro-binding energies for N1 protonation are greater than those for C3 protonation. This indicates that the N1−H···Y hydrogen bond is stronger when N1 is protonated, perhaps reflecting the more localized nature of the charge in this case.

B. Weak Acids: NH_4^+ to HF. The strongest of the weak acids are NH_4^+ and NH_3Me^+. Only a single complex, corresponding to proton transfer to N1, exists when these acids interact with vinylamine. These hydrogen-bond donors are small ions in which two N−H bonds provide a pathway for the conversion of a C3-complex to an N1-complex, as illustrated in Figure 11.

Interaction of vinylamine with the remaining weak acids listed in Table 4 leads to hydrogen-bonded complexes in which the acid is the proton donor to the lone pair at N1 or to C3 through the π system. Except for LiCNH$^+$ and NaCNH$^+$, the structures of the complexes are similar to the complexes of HF with vinylamine illustrated in Figure 8, with no proton transfer taking place. N1 is the preferred interaction site by 42.4 (LiCNH$^+$),

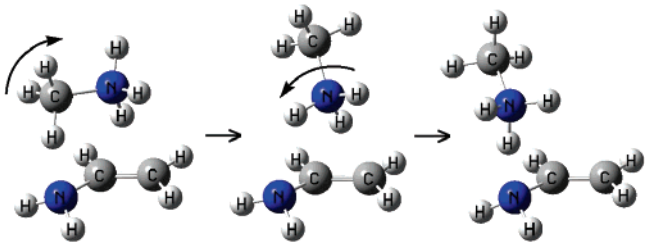

Figure 11. Selected structures observed during optimization of a C3-complex of vinylamine with NH_3Me^+. The additional N1−H bonds provide a pathway for the conversion of the C3-complex to an N1-complex.

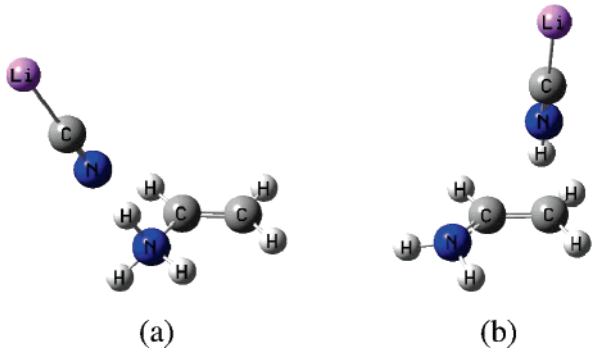

Figure 12. Complexes of vinylamine with LiCNH$^+$ (a) at N1 with proton transfer and (b) at C3 with no proton transfer.

9.5 ($NH_2Me_2^+$), 7.3 ($NHMe_3^+$), 27.5 (NaCNH$^+$), 9.7 (LiNCH$^+$), 5.8 (HBr), 6.8 (HCl), 9.5 (HNC), 3.8 (HCN), and 12.4 (HF) kJ mol^{-1}. Thus, the differences in the interaction energies at N1 and C3 are about 10 kJ mol^{-1} or less, except for complexes formed with LiCNH$^+$ and NaCNH$^+$.

Proton transfer occurs to N1 of vinylamine when LiCNH$^+$ and NaCNH$^+$ are the acids, even though the protonation energies of the conjugate bases of these acids (LiCN, −949.6 kJ mol^{-1}; NaCN, −997.9 kJ mol^{-1}) are greater than that of vinylamine at N1 (−884.9 kJ mol^{-1}). That is, full proton transfer at N1 by LiCNH$^+$ and NaCNH$^+$ is unfavorable by 64.7 and 113.0 kJ mol^{-1}, respectively, on the basis of protonation energies. This implies that the N1−H···N hydrogen-bond energies for the complexes with N1−H as the proton donor and LiCN and NaCN as the proton acceptors must more than compensate for the differences between the protonation energies of the bases and vinylamine at N1 in order that the proton transfer be favored. That such is the case can be seen from the retro-binding energies given in Table 4, which are −179.1 and −203.9 kJ mol^{-1}. The large retro-binding energies are linked to the large dipole moments of LiCN and NaCN, calculated to be 3.70 and 4.42 D, respectively, at the MP2/aug′-cc-pVTZ level. In the complexes with N1−H as the proton donor and LiCN or NaCN as proton acceptors, there is a strong electrostatic interaction resulting from a favorable head-to-tail alignment of the N1−H bond dipole with the dipole moments of these acceptors. Proton transfer does not occur at C3 because the resulting C3−H···N hydrogen bonds that would be formed with LiCN and NaCN are much weaker, and do not compensate for the difference in protonation energies, even though the C3 protonation energy of vinylamine (−941.7 kJ mol^{-1}) is similar to the protonation energy of LiCN (−949.6 kJ). The structures of the two complexes formed between LiCNH$^+$ and vinylamine are depicted in Figure 12. It is interesting to note that LiNC has an almost identical dipole moment to LiCN. However, its much larger protonation energy (−1018.7 kJ mol^{-1}) proves to be too

TABLE 5: MP2/aug′-cc-pVTZ//MP2/6-31+G(d,p) Binding Energies[a] for Complexes Formed between the Hydrogen-Bond Donors ($A-H^{n+}$) and Furan (kJ mol^{-1})[b]

	site of binding		
$H-A^{n+}$	O1	C2	C3
H^+	−702.2[c]	−816.7	−766.5[c]
$HF-H^+$	−266.1 (**−67.2**)[c]	−349.2 (**−35.8**)[c]	−300.2 (**−37.0**)
$HCl-H^+$	−189.2 (**−58.2**)[c]	−270.7 (**−25.2**)	−222.2 (**−26.8**)
$HBr-H^+$	−170.1 (**−63.9**)[c]	−247.8 (**−27.1**)	−192.5 (**−22.0**)
H_2O-H^+	−122.9 (**−132.2**)	−156.2 (**−51.0**)	−106.9 (**−51.8**)
$HCN-H^+$	−109.6 (**−134.4**)[c]	−141.0 (**−51.3**)	−96.2 (**−56.6**)
$HNC-H^+$	−68.6 (**−167.9**)[c]		−85.3 (**−120.1**)
H_3N-H^+	−65.1 (**−244.5**)[c]		−71.3 (**−186.3**)
$LiCN-H^+$	−59.0 (**−306.4**)[c]		−56.1 (**−239.2**)
$NaCN-H^+$	−52.4 (**−348.1**)[c]		−49.9 (**−281.2**)
$LiNC-H^+$	−38.4 (**−354.9**)[c]		−46.8 (**−299.0**)
Br−H	−18.1 (**−678.0**)[d]		−21.3 (**−616.8**)
Cl−H	−18.1 (**−717.0**)[d]		−19.3 (**−653.9**)
CN−H	−26.0 (**−735.6**)[c]		−25.4 (**−670.7**)
NC−H	−14.9 (**−798.9**)[c]		−19.3 (**−739.0**)
F−H	−25.9 (**−884.6**)[d]		−20.6 (**−814.9**)

[a] Binding energies in regular font are relative to furan plus $A-H^{n+}$, those in bold are relative to protonated furan at the corresponding atom plus $A^{(n-1)+}$. [b] The complexes have C_1 symmetry unless otherwise noted. [c] C_s. [d] C_{2v}.

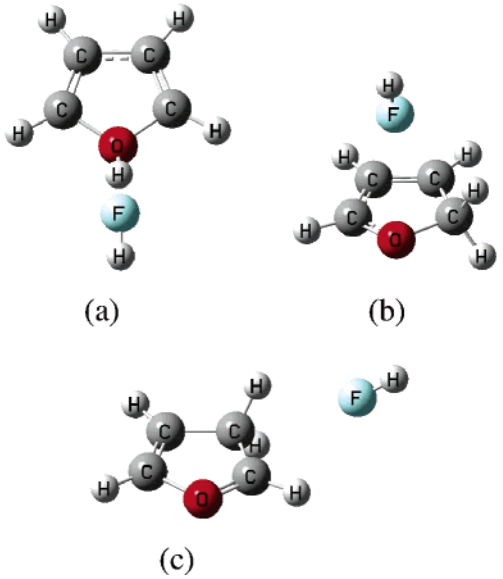

Figure 13. Complexes resulting from the reaction of furan with H_2F^+: (a) protonation at O1, with the formation of an O−H···F hydrogen bond, (b) protonation at C2, and (c) protonation at C3.

great an obstacle to overcome, and this prevents $LiNCH^+$ from transferring a proton to N1 of vinylamine.

In general, complexation energies for both N1 and C3 interaction sites decrease with decreasing acidity, as is clear from Figure 1 in going from (c) to (b) to (a). There are a small number of exceptions due to particular interactions, as pointed out above. In addition, hydrogen-bond energies with the proton donors HCN (N1 and C3) and HF (N1 and C3) also show binding energies that are greater than would be expected on the basis of acidity alone, i.e., there are small differences between the acidity order and the order of proton-donating ability for hydrogen-bond formation.

Reactions of Acids with Furan

The binding energies and retro-binding energies of complexes formed by the set of acids at O1, C2, and C3 of furan are presented in Table 5. As is observed for the interaction of acids with vinylamine, and in accordance with Figure 1, the binding energies generally become smaller with decreasing acidity of the protonating acid. As noted above in the discussion of hydrogen bonding with vinylamine, acids that are stronger than NH_4^+ (H_2F^+ to $LiClH^+$ in Table 4) transfer a proton to vinylamine. Since furan is a weaker base than vinylamine, it should be anticipated that the crossover for proton transfer takes place at a higher point on the acidity scale.

A. Strong Acids: H_2F^+, H_2Cl^+, and H_2Br^+. There are only three acids, namely, H_2F^+, H_2Cl^+, and H_2Br^+, that transfer a proton to furan (**J**) at all protonation sites. For these acids, the binding energies decrease in the order C2 > C3 > O1, which is the same order observed for protonation by H^+. When proton transfer occurs to C2 or C3, the conjugate base of the protonating acid forms a complex with protonated furan in which the halogen atom is located somewhere above the ring, with the H atom of the HX molecule pointing away from the ring. When proton transfer occurs from H_2X^+ to O1, then an O1−H···X hydrogen bond is formed. The three types of complexes formed with H_2F^+ are illustrated in Figure 13.

The O1-protonated complexes have greater retro-binding energies (−58.2 to −67.2 kJ mol^{-1}) than either of the π-complexes, suggesting that protonated O1 is a strong proton donor for the formation of a linear O1−H···X hydrogen bond. The retro-binding energies of complexes formed at C2 and C3 range from −22.0 to −37.0 kJ mol^{-1}. For a given acid, the differences in retro-binding energies between the C2- and C3-protonated complexes are small (<5.1 kJ mol^{-1}).

B. Moderately Strong Acids: H_3O^+ and $HCN-H^+$. The complexes formed between furan and H_3O^+ or $HCN-H^+$ are not always those expected on the basis of the protonation energies of furan (−816.9, −766.5, and −702.2 kJ mol^{-1}, respectively, at C2, C3, and O1) and the conjugate bases H_2O (−711.3 kJ mol^{-1}) and HCN (−727.2 kJ mol^{-1}). Thus, it might have been expected that both acids should transfer a proton to furan at C2 and C3, but not at O1. However, only when these two acids interact with furan at C2 are the expected proton-transferred complexes observed, and these complexes have the largest binding energies. The C2-protonated complex with H_2O is structurally similar to the complexes formed at C2 by the strong acids. The complex formed with $HCN-H^+$ is stabilized by an essentially linear C2−H···N hydrogen bond. In contrast, neither H_3O^+ nor $HCN-H^+$ transfer a proton to furan at C3. Rather, the resulting complexes have these two acids as proton donors to furan through the π-system at C3. The complexes with H_3O^+ and $HCN-H^+$ are shown in Figure 14.

When H_3O^+ and $HCN-H^+$ interact with furan at O1, complexes with proton-shared hydrogen bonds are formed. In the case of H_3O^+, a nearly symmetric proton-shared O1···H···O hydrogen bond is formed, with O1···H and H···O distances of 1.176 and 1.213 Å, respectively. With $HCN-H^+$, a proton-shared hydrogen bond is again formed, with O1···H and H···N distances of 1.135 and 1.332 Å, respectively. The structures of these complexes are also included in Figure 14. When furan interacts with these two acids, the order of interaction energies differs from that for the protonation energies, decreasing in the order C2 > O1 > C3.

The retro-binding energies for the C2-complexes with H_3O^+ and $HCN-H^+$ are −51.0 and −51.3 kJ mol^{-1}, respectively, significantly greater than those of the C2-complexes with the strong acids. Even more dramatic are the retro-binding energies of the complexes formed at O1, which are −132.2 and −134.4 kJ mol^{-1} when the acids are H_3O^+ and $HCN-H^+$, respectively. The large retro-binding energies of the O1-complexes may be

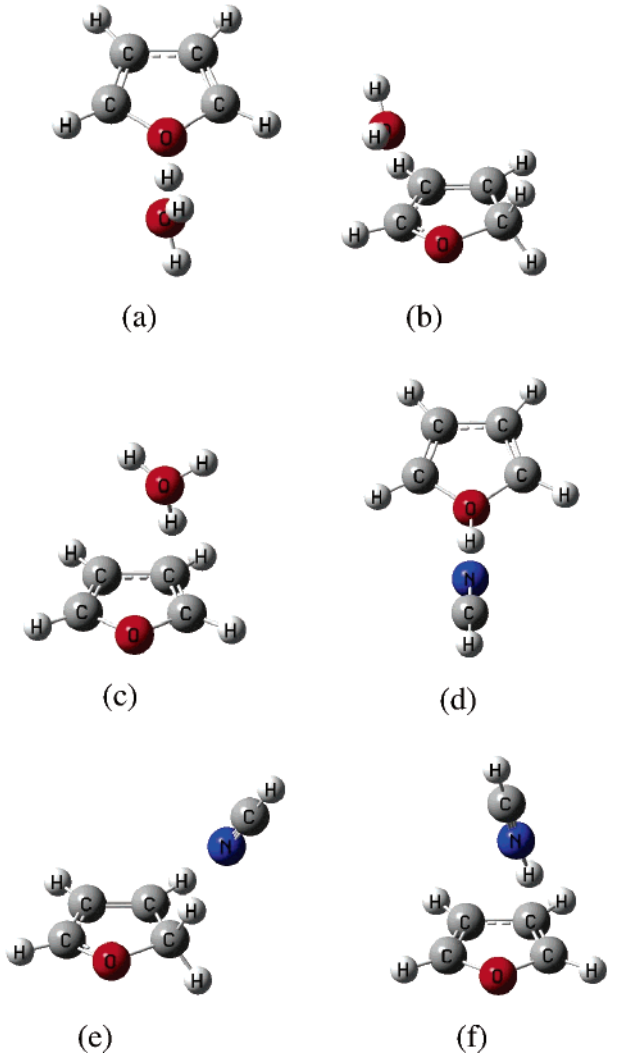

Figure 14. Complexes resulting from the reaction of furan with H_3O^+ (a) at O1, (b) at C2, and (c) at C3, and with $HCN{-}H^+$ (d) at O1, (e) at C2, and (f) at C3.

attributed to the similarity of the protonation energies of H_2O, HCN, and furan at O1, and hence the formation of very strong cationic O1···H···O and O1···H···N proton-shared hydrogen bonds in the complexes, reflective of the situation in Figure 1b.

C. Weak Acids: HNC−H$^+$ to HF. The weak acids do not transfer or share a proton with furan but form hydrogen bonds with the π-system at C3 or with the ring oxygen. The structures of the complexes formed between furan and $LiCNH^+$ are illustrated in Figure 15 as representative examples. It is interesting to note that when the hydrogen bond is formed at O1, most complexes do not have C_{2v} symmetry since the proton-donor molecule does not lie in the symmetry plane of the furan ring. Only when the hydrogen halides HF, HCl, and HBr are the proton donors do the resulting complexes have C_{2v} symmetry.

The weak acids can be subdivided into cationic and neutral proton donors for hydrogen bonding. The complexes with cations as proton donors are more stable than those with neutral donors. Cationic complexes have binding energies that range from −38.4 to −68.8 kJ mol^{-1} for complexes formed at O1, and from −46.8 to −85.3 kJ mol^{-1} for the C3-complexes. The neutral complexes formed at O1 have binding energies ranging from −14.9 to −25.9 kJ mol^{-1}, while those of the C3-complexes vary from −19.3 to −25.4 kJ mol^{-1}. In general, the binding energies of complexes at O1 and C3 decrease as the protonation energies of the conjugate bases of the acids increase. The exceptions are the complexes with HNC and HF, which have binding energies slightly greater than anticipated.

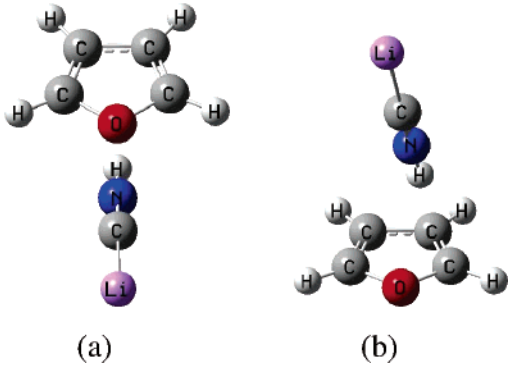

Figure 15. Hydrogen-bonded complexes of furan with $LiCNH^+$: (a) at O1 and (b) at C3.

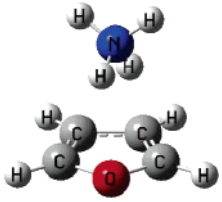

Figure 16. Complex between furan and NH_4^+ through the π-system, two hydrogen bonds being formed at C3 and at O1 through two $N{-}H{\cdots}\pi$ bonds.

The energy differences between the O1- and C3-complexes formed with the weak acids vary from 2.5 kJ mol^{-1} for $NaCNH^+$ to 16.7 kJ mol^{-1} mol^{-1} for $HNC{-}H^+$. Whether the O1- or the C3-complex is more stable depends on the proton donor. When the donor is NH_4^+, HCl or HBr, or a C−H donor ($HNC{-}H^+$ and $LiNCH^+$), the complex formed through the π-system is more stable. On the other hand, the O1-complex is more stable when the proton donor is HF or an N−H donor ($LiCNH^+$ and $NaCNH^+$). The complexes with NH_4^+ are an exception to this latter generalization since the unique structure of the C3 π-complex with two $N{-}H{\cdots}\pi$ hydrogen bonds gives it added stability. This complex is shown in Figure 16.

Conclusions

Ab initio molecular orbital calculations have been employed to investigate the relationship between the very important processes of protonation and hydrogen bonding. In the first part of this study, interactions between a set of bases with H^+ and HF were investigated. The second part involved a study of the complexes formed when acids of varying strengths interact with two of the bases, vinylamine and furan. These interactions all lead to protonation and/or hydrogen bonding. From this investigation, the following important points have emerged.

(1) Cyclopropenyl anion (**A**), cyclobutadiene (**B**), formamidine (**C**), formamide (**H**), malonaldehyde (**I**), 1,3-butadiene (**K**), and formic acid (**L**) preferentially protonate and form complexes with HF at the same basic site within the molecule, whereas the preferred sites for protonation and hydrogen bonding with HF are different for 1*H*-azirine (**D**), vinylamine (**E**), azete (**F**), pyrrole (**G**), and furan (**J**).

(2) The preferred site for protonation of the substrates listed above appears to be determined primarily by the ability of the protonated species to delocalize the acquired positive charge. On the other hand, localization of a pair of electrons at a proton-

acceptor site in the basic substrate tends to be more important in determining the preferred site for hydrogen bonding with HF.

(3) Consistent with a previously proposed Hammond postulate for complexes, when a substrate (B) interacts with acids (HA^+), proton transfer occurs when the proton affinity of A is significantly less than that of the substrate, to produce the complex $A\cdots{}^+H-B$. When the proton affinity of A is greater than that of B, a hydrogen-bonded complex ($A-H^+\cdots B$) is generally formed without proton transfer. When A and B have similar proton affinities, then whether proton transfer occurs, and what type of complex is formed, depends on the relative proton affinities and on the strengths of the resulting hydrogen bonds that stabilize the complex.

(4) For vinylamine, proton transfer occurs in some cases when this would not be predicted on the basis of protonation energies alone, as a consequence of specific interactions in the resulting complexes.

(5) For furan, when the protonation energies of the conjugate bases of the acids approach those of furan, proton transfer occurs at C2 as expected, but it does not occur at C3 even when the protonation energy of furan at this site is somewhat greater than that of the conjugate bases of the acids. Interaction at O1 leads to partial proton transfer, and the formation of hydrogen-bonded complexes stabilized by strong proton-shared hydrogen bonds.

Acknowledgment. We gratefully acknowledge generous allocations of computing time from the Ohio Supercomputer Center, the National Facility of the Australian Partnership for Advanced Computing (APAC), the Australian National University Supercomputing Facility (ANUSF), and the Australian Center for Advanced Computing and Communications (AC3), the provision (to B.C.) of a New Zealand Science & Technology Post-Doctoral Fellowship by the Foundation for Research, Science & Technology, the award (to J.E.D.B.) of a Visiting Professorship at the University of Sydney, and the provision of grants by the U.S. National Science Foundation (NSF CHE-9873815 to J.E.D.B.), Spanish DGI/MCyT (project no. BQU-2003-01251 to J.E.), and the Australian Research Council (DP0342529 and DP0556706 to L.R.).

Supporting Information Available: GAUSSIAN 03 archive entries for MP2/6-31+G(d,p)-optimized geometries of relevant equilibrium structures, calculated MP2/aug′-cc-pVTZ electronic energies, and full citation for ref 16. This material is available free of charge via the Internet at http://pubs.acs.org.

References and Notes

(1) For recent reviews, see: (a) Jeffrey, G. A. *An Introduction to Hydrogen Bonding*; Oxford University Press: New York, 1997. (b) Desiraju, G. R.; Steiner, T. *The Weak Hydrogen Bond. IUCr Monographs on Crystallography*; Oxford University Press: New York, 1999; p 21. (c) Scheiner, S. *Hydrogen Bonding. A Theoretical Perspective*; Oxford University Press: New York, 1997; p 61. (d) Scheiner, S. *Molecular Interactions. From van der Waals to Strongly Bound Complexes*; John Wiley and Sons: Chichester, UK, 1997; p 164.

(2) (a) Gal, J.-F.; Maria, P.-C. *Prog. Phys. Org. Chem*. **1990**, *17*, 159 (see p 209). (b) Graton, J.; Berthelot, M.; Laurence, C. *J. Chem. Soc., Perkin Trans. 2* **2001**, 2130.

(3) (a) Legon, A. C.; Rego, C. A. *J. Chem. Phys*. **1989**, *90*, 6867. (b) Legon, A. C.; Wallwork, A. L.; Rego, C. A. *J. Chem. Phys*. **1990**, *92*, 6397. (c) Legon, A. C. *Chem. Soc. Rev*. **1993**, *22*, 153. (d) Legon, A. C. *J. Chem. Soc., Chem. Commun*. **1996**, 109. Barnes, A. J.; Legon, A. C. *J. Mol. Struct*. **1998**, *448*, 101. (e) Cooke, S. A.; Corlett, G. K.; Lister, D. G.; Legon, A. C. *J. Chem. Soc., Faraday Trans.* **1998**, *94*, 837.

(4) Latajka, Z.; Scheiner, S.; Ratajczak, K. *Chem. Phys*. **1992**, *166*, 85.

(5) (a) Perchard, J. P. In *Matrix-Isolation Spectroscopy*; Barnes, A. J., Orville-Thomas, W. J., Müller, Gaufrès, R., Eds.; NATO Advanced Study Institute; Reidel: Dordrecht, The Netherlands, 1981; pp 551−563. (b) Barnes, A. J. *J. Mol. Struct.* **1983**, *100*, 259. (c) Andrews, L. In *Chemistry and Physics of Matrix-Isolated Species*; Andrews, L., Moskovits, M., Eds.; North-Holland: Amsterdam, The Netherlands, 1989; pp 15−46. (d) Maes, G. In *Intermolecular Forces. An Introduction to Modern Methods and Results*; Huyskens, P. L., Luck, W. A. P., Zeegers-Huyskens, Th., Eds.; Springer: Berlin, Germany, 1991; pp 195−216.

(6) (a) Jacox, M. E. *J. Phys. Chem. Ref. Data* **1994**, Monograph No. E. (b) Szczepaniak, K.; Chabrier, P.; Person, W. B.; Del Bene, J. E. *J. Mol. Struct*. **2000**, *520*, 1.

(7) (a) Shenderovich, I. G.; Burtsev, A. P.; Denisov, G. S.; Golubev, N. S.; Limbach, H.-H. *Magn. Res. Chem*. **2001**, *39*, S91. (b) Golubev, N. S.; Shenderovich, I. G.; Smirnov, S. N.; Denisov, G. S.; Limbach, H.-H. *Chem. Eur. J*. **1999**, *5*, 492.

(8) (a) Del Bene, J. E.; Bartlett, R. J.; Elguero, J. *Magn. Res. Chem*. **2002**, *40*, 767. (b) Del Bene, J. E. In *Calculation of NMR and EPR Parameters*; Kaupp, M., Bühl, M., Malkin, V., Eds.; Wiley-VCH: Weinheim, Germany, 2004; pp 353−370.

(9) (a) Chipot, C.; Rinaldi, D.; Rivail, J.-L. *Chem. Phys. Lett*. **1992**, *191*, 287. (b) Alkorta, I.; Rozas, I.; Mó, O.; Yáñez, M.; Elguero, J. *J. Phys. Chem. A* **2001**, *105*, 7481. (c) Mó, O.; Yáñez, M.; González, L.; Elguero, J. *Chem. Phys. Chem*. **2001**, 465.

(10) (a) Smith, D. M.; Golding, B. T.; Radom, L. *J. Am. Chem. Soc.* **1999**, *121*, 5700. (b) Smith, D. M.; Golding, B. T.; Radom, L. *J. Am. Chem. Soc.* **2001**, *123*, 1664. (c) Wetmore, S. D.; Smith, D. M.; Golding, B. T.; Radom, L. *J. Am. Chem. Soc.* **2001**, *123*, 7963.

(11) (a) Maiti, N.; Widjaja, L.; Banerjee, R. *J. Biol Chem.* **1999**, *274*, 32733. (b) Thomä, N.; Evans, P. R.; Leadlay, P. F. *Biochemistry* **2000**, *39*, 9213. (c) Madhavapeddi, P.; Marsh, E. N. G. *Chem. Biol*. **2001**, *8*, 1143.

(12) (a) Bürgi, H.-B.; Dunitz, J. D. *Acc. Chem. Res*. **1983**, *16*, 153. (b) Bürgi, H.-B.; Dunitz, J. D. *Structure Correlation*; VCH: Weinheim, Germany, 1994; Vol. 1, p 197.

(13) (a) Bouma, W. J.; Radom, L. *Chem. Phys. Lett.* **1979**, *64*, 216. (b) Pross, A.; Radom, L. *J. Am. Chem. Soc.* **1981**, *103*, 6049. For the original Hammond postulate formulated for transition structures, see: (c) Hammond, G. S. *J. Am. Chem. Soc.* **1955**, *77*, 334.

(14) For recent studies of the protonation of these species, see, for example: (a) van Beelen, E. S. E.; Koblenz, T. A.; Ingemann, S.; Hammerum, S. *J. Phys. Chem. A* **2004**, *108*, 2787. (b) Maksic, Z. B.; Vianello, R. *J. Phys. Chem. A* **2002**, *106*, 419. (c) Álvarez, G.; Palomar, J.; de Paz, J. L. G. *THEOCHEM* **2001**, *541*, 111. (d) Maksic, Z. B.; Kovacevic, B.; Lesar, A. *Chem. Phys.* **2000**, *253*, 59. (e) Merrill, G. N.; Kass, S. R. *J. Am. Chem. Soc.* **1997**, *119*, 12322. (f) Bagno, A.; Scorrano, G. *J. Phys. Chem.* **1996**, *100*, 1536. (g) Nguyen, V. Q.; Turecek, F. *J. Mass Spectrom.* **1996**, *31*, 1173. (h) Berger, D. J.; Gaspar, P. P.; Liebman, J. F. *THEOCHEM* **1995**, *338*, 51. (i) Tortajada, J.; Leon, E.; Morizur, J.-P.; Luna, A.; Mó, O.; Yáñez, M. *J. Phys. Chem.* **1995**, *99*, 13890 and references therein.

(15) See for example: (a) Hehre, W. J.; Radom, L.; Schleyer, P. v. R.; Pople, J. A. *Ab Initio Molecular Orbital Theory*; Wiley: New York, 1986. (b) Jensen, F. *Introduction to Computational Chemistry*; Wiley: Chichester, UK, 1998. (c) Koch, W.; Holthausen, M. C. *A Chemist's Guide to Density Functional Theory*, 2nd ed.; Wiley: New York, 2001.

(16) Frisch, M. J.; et al. *Gaussian 03*, Revision B.03; Gaussian, Inc.: Pittsburgh, PA, 2003.

(17) (a) Del Bene, J. E. *J. Phys. Chem.* **1993**, *97*, 107. (b) Del Bene, J. E. In *The Encyclopedia of Computational Chemistry*; Schleyer, P. v. R., Allinger, N. L., Clark, T., Gasteiger, J., Kollman, P. A., Schaefer, H. F., III, Schreiner, P. R., Eds.; John Wiley & Sons: Chichester, UK, 1998; Vol. 2, pp 1263−1271. (c) Dunning, T. H., Jr. *J. Phys. Chem. A* **2000**, *104*, 9062. (d) Valdes, H.; Sordo, J. A. *J. Phys. Chem. A* **2003**, *107*, 899.

(18) Scott, A. P.; Radom, L. *J. Phys. Chem.* **1996**, *100*, 16502.

(19) Linstrom, P. J.; Mallard, W. G., Eds. *NIST Chemistry WebBook*; NIST Standard Reference Database No. 69; National Institute of Standards and Technology: Gaithersburg MD, 20899, March 2003 (http://webbook.nist.gov).

(20) See, for example: Smith, B. J.; Radom, L. *Chem. Phys. Lett.* **1994**, *231*, 345.